1st International Conference on the Material Point Method, MPM 2017

Granular column collapse of wet sand

Elliot J. Fern[a], Kenichi Soga[a]

[a]*University of Cambridge, Department of Engineering, Trumpington Street, Cambridge CB2 1PZ, United Kingdom*

Abstract

It is well known that partial saturation enhances the mechanical behaviour of sand. Whilst its influence at small deformation has been largely discussed in the literature, its influence at large deformation remains largely unexplored. This paper investigates the influence of partial saturation on the collapse and flow of dry and wet sand by simulating a well established experiment, called the *granular column collapse*, using the material point method. The results showed that partial saturation influences the primary failure surface at small deformation, which defined the volume of the mobilised mass, the post-failure flow behaviour and the run-out distance, though not as significantly as one could expect. This can be explained by small differences in the potential energy of the mobilised mass as it will be explained in this paper.

1. Introduction

The granular column collapse is a well established experiment, which consists in releasing a column of granular material on a flat surface, and extensive data is available in the literature covering a variety of dry granular materials [1–5]. Whilst the the experiment offers simplicity in execution, its numerical simulation is complex [6] due to transition from solid-like to fluid-like behaviours and the low stresses. A variety of numerical methods have been used to simulate the column collapse such as MPM [7–11], DEM [8,12] or SPH [7,13]. However, most continuum methods relied on simple constitutive models to idealise the mechanical behaviour of the dry sand. Fern and Soga [14] showed that these simple constitutive models overestimated the run-out distance due to insufficient energy dissipation but more advanced models, such as Nor-Sand [15], could predict the correct run-out distance for dry sand. However, the failure and flow mechanism of wet sand have never been investigated. Yerro et al. [16] investigated the failure mechanism of progressive landslides in partially saturated conditions with MPM but did not investigate the flow behaviour. Bandara [7] investigated the collapse and flow of partially saturated levees but used a simple Mohr-Coulomb model. The ability of MPM to model slope failures has been discussed by Soga et al. [17].

---

* Corresponding author.
  E-mail address: jf497@cam.ac.uk

Fern et al. [18] showed that the enhancement by partial saturation of the mechanical behaviour of sand can be explained by a modification of the soil fabric and, hence, a modification of the dilatancy characteristics. This modelling approach offers an advantage when modelling the transition from small strain solid-like to large strain flow-like behaviours as the contribution of dilatancy towards strength is automatically mitigated as the material reaches the critical state [19].

The combination of the recent developments in MPM simulations along with the development in constitutive models allows investigating the failure and post-failure behaviours of wet sand. Following the same path as Fern and Soga [14], two columns collapses were simulated for dry and wet sand, respectively. Additionally, the potential energy of the mobilised mass, which can be used as a proxy for the run-out distance, was computed for two different densities and for two different degrees of saturation.

2. Constitutive modelling of wet sand - Unsaturated Nor-Sand

There is a consensus among the scientific community that constitutive models for unsaturated soils are extensions of saturated models. Therefore, the abilities and limitations of a given model to predict the mechanical behaviour of saturated soil will be inherited in the unsaturated extension. For instance, the Barcelona Basic Models [20] suffers from the same limitations, when modelling dense soils, as the Cam-Clay models [19,21] as discussed by Fern [22]. Moreover, constitutive models for large deformation simulations must be able to capture both the small strain and the large strain behaviours. This is paramount as the initial failure surface and, hence, the mobilised mass are defined at small strains whilst the flow takes place at large deformation. The critical state soil mechanics framework [23] offers an ideal framework in which such a model can be developed.

2.1. Critical State

Roscoe et al. [24] suggested that any soil sheared sufficiently would eventually reach a unique state called the *critical state* at which point the dilatancy rate and the changes in dilatancy rate are nil (Eq. 1).

$$D = \frac{\partial D}{\partial \varepsilon_d} := 0 \tag{1}$$

where $D = d\varepsilon_v / \partial \varepsilon_d$ is the dilatancy rate, ε_v the volumetric strain and ε_d the deviatoric strain.

Roscoe and Schofield [21] were driven by Taylor's idea [25] that the strength of soil was the consequence of intergranular friction and interlocking. They expressed the stress-dilatancy theory in terms of stress and strains invariants. An additional dilatancy parameter N was later introduced [26] to offer better modelling possibilities (Eq. 2)

$$\eta' = M + (N - 1)D \tag{2}$$

where $\eta' = q/p'$ is the effective stress ratio, p' the mean effective stress, q the deviatoric stress, M the critical state effective stress ratio and N the dilatancy parameter, which is nil in the Cam-Clay models ($N = 0$).

Therefore, the nil dilatancy condition of the critical state theory and the stress-dilatancy theory imply that a unique stress state exists at the critical state (Eq. 3).

$$D = 0 \rightarrow \eta'_{cs} = M \tag{3}$$

Bolton [27] suggested a state index called the *relative dilatancy index* as a proxy for dilatancy. Boulanger [28], followed by Mitchell and Soga [29], showed that the relative dilatancy index could be used to define the critical state density as the dilatancy rate is nil (Eq. 4).

$$I_R = I_D \cdot I_C - 1 = 0 \rightarrow e_{cs} = e_{max} - \frac{e_{max} - e_{min}}{\ln(Q/p')} \tag{4}$$

where I_R is the relative dilatancy index, $I_D = (e_{max} - e)/(e_{max} - e_{min})$ with e_{max} and e_{min} the maximum and minimum void ratios, $I_C = \ln(Q/p')$ the relative pressure index with the Q the crushing pressure, which is typically 10 MPa for silica sand, and e_{cs} the critical state void ratio.

Fern [22] showed that this non-linear critical state line was valid for 10 different sands and that the critical state line, as suggested by Roscoe et al. [24], did not have to be a modelling assumption but could be predicted from the relative dilatancy index (Eq. 4). Moreover, Fern et al. [18] showed that the stress-dilatancy theory was still valid for partially saturated sand and that Eqs. 3 and 4 could be used.

2.2. Constitutive model for sand in large deformation simulations

Cam-Clay [19,21] couples the two conditions of the critical state theory ($D = 0 \leftrightarrow \partial D/\partial \varepsilon_d = 0$). Therefore, these models cannot distinguish the phase transition point ($\eta' = M$, $D = 0$ but $\partial D/\partial \varepsilon_d \neq 0$) [30,31], which is the end of the contractive phase and start of the dilative phase of dense soil, from the critical state ($\eta' = M$, $D = \partial D/\partial \varepsilon_d = 0$). For this reason, these models were restricted to contractive soils [32]. However, it is possible to model the peak state as a yielding point by introducing the concept of preconsolidation but is inconsistent with the stress-dilatancy theories [25,33]. The preconsolidation pressure sizes the yield surface and determines the peak strength but remains a modelling assumption.

Nor-Sand [15], among other models)(i.e. SaniSand [34]), decouples the two conditions of the critical state theory by having two yield surfaces - the yield surface which determines the elastic domain and the maximum yield surface which determines the peak state. The decoupling of the two conditions allows the distinction between the phase transition point ($\eta' = M$, $D = 0$ but $\partial D/\partial \varepsilon_d \neq 0$) and the critical state ($\eta' = M$, $D = \partial D/\partial \varepsilon_d = 0$) to be made. Therefore, the hardening phase is elasto-plastic and energy is dissipated. The peak state is determined from the dilatancy characteristics which allows the model to include the void ratio as a model variable. This is important for large deformation simulations as the initial density can differ substantially from the final one. Furthermore, the estimation of the peak strength from dilatancy characteristics allows the model to take its contribution into account at small strains whilst excluding it at large strains.

Nor-Sand predicts the mechanical behaviour of sand from its density and its dilatancy characteristics. However, it cannot differentiate between sand which has been previously sheared and one which has not. In large deformation simulation of flowing sand, it is possible for the largely sheared sand to undergo a sudden increase in density, which results in an 'explosion' of material points. this can be prevented by introducing a strain-history variable such as the accumulated plastic deviatoric strain E_d^p [22]. A condition is then implemented in the model such that dilatancy is prevented for accumulated plastic deviatoric strain exceeding a given value $E_{d,\psi=0}^p$ (Eq. 5). This is a major difference between the implementation of the model for FEM and MPM.

$$\psi := 0 \quad for \quad E_d^p > E_{d,\psi=0}^p \tag{5}$$

where ψ is the state parameter [35] and the accumulated plastic strain cut-off is $E_{d,\psi=0}^p = 100\%$ in the following simulations.

Fern et al. [18] showed that partial saturation enhances the dilatancy characteristics and that the minimum dilatancy rate can be predicted from state indices such as the state parameter ψ (Eq. 6) [35].

$$D_{min} = \chi_{(S_w)} \cdot \psi \tag{6}$$

where D_{min} is the minimum dilatancy rate which occurs at peak state, $\chi_{(S_w)}$ the dilatancy coefficient which is a function of the soil fabric and partial saturation S_w, and ψ the state parameter which is a function of the density and pressure.

The yield surface is enhanced by partial saturation for stress-relaxation reasons [22]; it is a decrease of stress by wetting and with no changes in volume. The maximum yield surface is enhanced by partial saturation because of an enhancement of the dilatancy characteristics in a similar way it is for the Barcelona Basic Model [20,36]. A complete description of the model is given in Fern et al. [18].

3. MPM simulations of column collapses of wet sand

Two simulations of the column collapse with an initial aspect ratio of 2.0 were carried out with Anura 3D. The layout of the model was identical to the one presented in Fern and Soga [14]. The columns were filled with dry and wet sand, respectively. Partial saturation was modelled as a state variable of the material points and the simulations were run with the 1-layer 1-phase formulation. This was motivated by the flow behaviour in which the water is transported
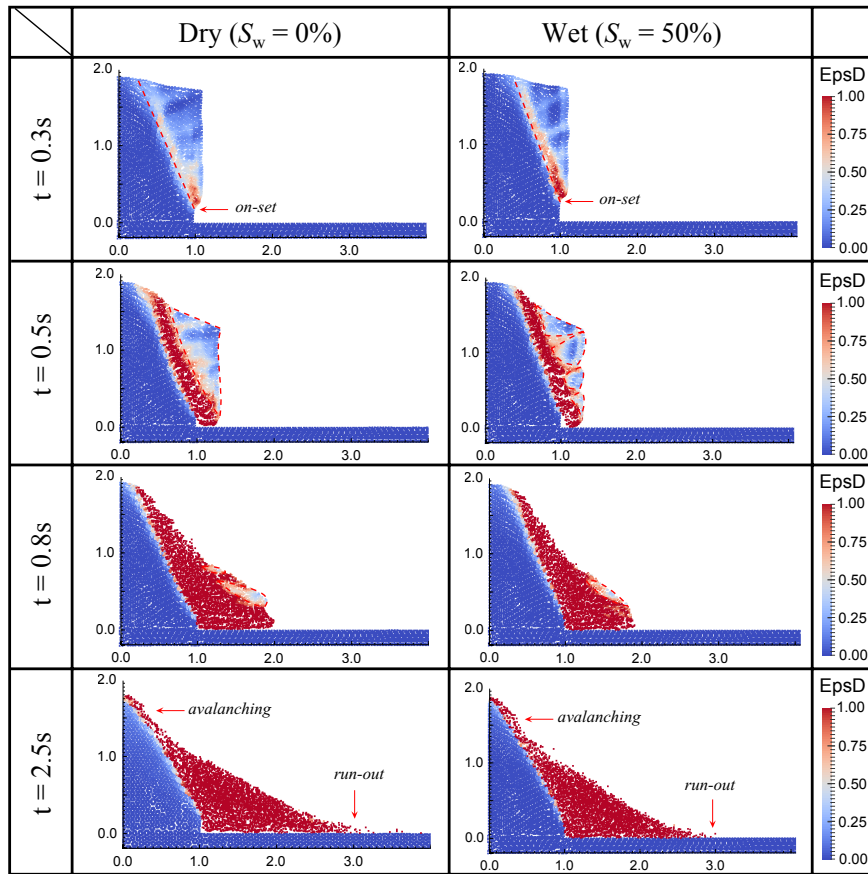
Fig. 1. MPM simulation of column collapse of dry and wet sand.

Table 1. Unsaturated Nor-Sand model parameters and initial state.

A	n	ν	M_{tc}	N	N_f	e_{min}	e_{max}	Q	H	χ_{sat}	$\Delta\chi_{max}$	Δp_i	β_{wet}	β_{wet}	e_0	$S_{w,0}$
2500	0.3	0.2	1.33	0.3	0.6	0.500	0.946	10 MPa	25 -1850ψ	2.6	4.0	1 kPa	3.5	0.5	0.8	0%, 50%

where $G = A p'^n$ is the elastic shear modulus with A the elastic modulus constant and n the elastic modulus exponent, ν the Poisson ratio, M_{tc} the triaxial compression critical state effective stress ratio, N the dilatancy parameter of the potential function, N_f the dilatancy parameter of the yield function, H the hardening modulus, ψ the state parameter, χ_{sat} the saturated dilatancy coefficient, $\Delta\chi_{max}$ the maximum enhancement by partial saturation of the dilatancy coefficient, Δp_i the enhancement by partial saturation of the image pressure, β_{wet} and β_{wet} the shape function below and above the residual degree of saturation respectively, e_0 the initial void ratio and $S_{w,0}$ the initial degree of saturation.

with the solid material in the same velocity field. This approach was significantly computationally cheaper than solving all the governing equation in the 1-layer 3-phase formulation [16] and avoided some limitations with the boundary conditions due to the flowing mass.

The simulations were carried out for loose sand ($e_0 = 0.80$, $I_D = 33\%$) and with the non-associative formulation of Unsaturated Nor-Sand [18]. The initial model parameters and states are given in Table 1.

The results of the simulations are shown in Fig. 1. The results show the formation of the slip surface (t = 0.3 s). Once this slip surface was fully developed, a wedge was formed and defined the mobilised mass. Partial saturation enhanced the mechanical properties of the sand and, thus, the slope of the slip surface was steeper and the on-set point

of the slip surface was located at a higher position for the wet sand than for the dry one. The mobilised mass was smaller for the wet sand than for the dry one, though limited. The results show that the way the wedge slide on the slip surface was different for the dry and the wet sands. The dry sand wedge slide as a block (t = 0.5 s) and crumbled upon contact with the basal layer. The wet sand wedge slid in a blocky manner. Bandara [7,17] observed a similar behaviour when modelling the collapse of a partially saturated levees. This is a consequence of the enhanced dilatancy characteristics of unsaturated sand. These blocks then crumbled upon contact with the basal layer and a multi-layer flow started (t = 0.8 s) for both the dry and the wet sand. At this stage, the entire mobilised mass had reached the critical state and the enhanced dilatancy characteristics did not play any role. The inter-granular friction, defining the critical state friction angle, slowed the flow progressively down. Static layers of sand were built bottom up until the final run-out distance was reached (t = 2.5 s). The results suggests that the run-out distance were within the same range for both the dry and the wet sand. However, the final height were somewhat different. Towards the end of the simulations, an avalanching process started at the summit of the static cone; that is the part of the column which was not initial mobilised. The avalanching process is consistent with experimental observation [3,4] and other numerical investigations of slope failures [37]. It was more significant for the wet sand than for the dry one.

The results of the MPM simulations of wet and dry sand granular column collapses suggest that partial saturation modifies the development of the slip surface but does not significantly influence the run-out distance.

4. Discussion

Fern and Soga [14] suggested that the run-out distance was governed by the amount of energy of the mobilised mass (Eq. 7) and showed that the initial potential energy can be calculated (Eqs. 8-9). Two types of collapsing behaviours were observed in the experiments [1–5] and are related to the size of the column - small and large aspect ratio columns (Fig. 2). The transition from one to the other was found to be density and material dependent [18].

$$E_{pot}^{mob}(t = 0s) = E_{pot}^{mob}(t) + E_{kin}^{mob}(t) + dissipation(t) \tag{7}$$

- for small aspect ratios:

$$E_{pot}^{mob}(t = 0s) = \frac{1}{3}h_0^3 \cot \varphi'(1 - n)\rho_s g \tag{8}$$

- for large aspect ratios:

$$E_{pot}^{mob}(t = 0s) = \left(\frac{1}{2}h_0^2 r_0 - \frac{1}{6}r_0^3 \tan^2 \varphi'\right)(1 - n)\rho_s g \tag{9}$$

where E_{pot}^{mob} and E_{kin}^{mob} are the potential and kinetic energies of the mobilised mass, t the time, h_0 the height of the column, r_0 the radius of the column, φ' the friction angle, n the porosity, ρ_s the unit mass of the dry sand and g the gravity.
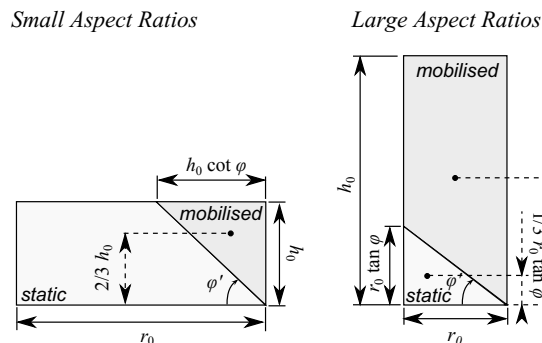

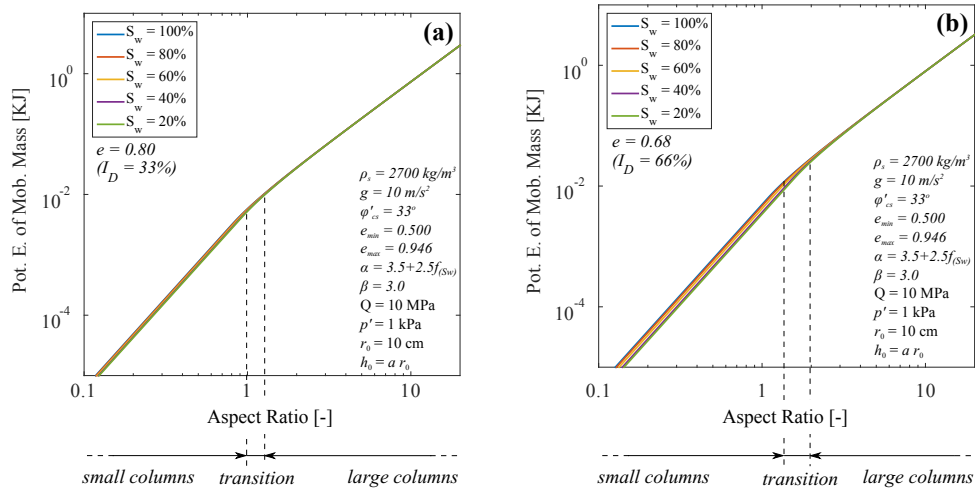Fig. 2. Definition of mobilised mass in small and large columns, after [14].

Fig. 3. Potential energy of mobilised mass: (a) loose sand and (b) dense sand.

Fern et al. [22] showed the friction peak strength, from which the friction angle was obtained, can be estimated from the relative dilatancy index [27] (Eqs. 10-12).

$$\varphi' = \varphi_{cs} + \psi_{max} \tag{10}$$

$$\psi_{max} = \alpha_{(S_w)} I_R \tag{11}$$

$$\alpha_{(S_w)} = \alpha_{sat} + \Delta\alpha_{max} \cdot f_{(S_w)} \tag{12}$$

where ψ_{max} is the maximum dilatancy angle, $\alpha_{(S_w)}$, α_{sat} and $\Delta\alpha_{max}$ the dilatancy coefficient, the saturated dilatancy coefficient and the maximum enhancement of the dilatancy coefficient, respectively, and $f_{(S_w)}$ the shape function defined in [18]. The dilatancy coefficient were calibrated on direct shear tests [38] and the dilatancy coefficient were found to be $\alpha_{sat} = 3.5$, $\Delta\alpha_{max} = 2.5$ and $\beta = 3.0$ (see [18] for definitions).

Fig. 3 (a) and (b) show the potential energy of the mobilised mass for loose and dense sand, respectively. The results suggests that partial saturation mainly affects small columns and that its influence is density dependent. The influence of partial saturation is similar to the one of density, though not as significant.

5. Conclusion

The results of the MPM simulations show that the collapsing behaviour was influenced by partial saturation. The slip surface was steeper, the mobilised mass smaller, albeit limited, and the flow behaviour was blocky. These observations are consistent with previous investigation using simple constitutive models [17] but for which the run-out distance of fluid-like behaviours would be over-estimated; this is not the case for sliding behaviours for which energy is only dissipated on the slip surface. The MPM simulations also show that the run-out distance was not significantly influenced by partial saturation. The analysis of the potential energy confirmed the limited influence of partial saturation on the run-out distance. However, it also showed that the influence was more significant for dense soils and small columns than for loose once and large columns.

Acknowledgements

References

[1] E. Lajeunesse, A. Mangeney-Castelnau, J. P. Vilotte, Spreading of a granular mass on a horizontal plane, Physics of Fluids 16 (2004) 2371–2381.

[2] E. Lajeunesse, J. B. Monnier, G. M. Homsy, Granular slumping on a horizontal surface, Physics of Fluids 17 (2005) 103302.

[3] G. Lube, H. Huppert, R. Sparks, M. Hallworth, Axisymmetric collapses of granular columns, Journal of Fluid Mechanics 508 (2004) 175–199.

[4] G. Lube, H. E. Huppert, R. S. J. Sparks, A. Freundt, Collapses of two-dimensional granular columns, Physical Review E - Statistical, Nonlinear, and Soft Matter Physics 72 (2005) 1–10.

[5] G. Lube, H. Huppert, R. S. J. Sparks, A. Freundt, Static and flowing regions in granular collapses down channels, Physics of Fluids 19 (2007) 043301.

[6] O. Pouliquen, Scaling laws in granular flows down rough inclined planes, Physics of Fluids 11 (1999) 542–548.

[7] S. Bandara, Material point method to simulate large deformation problems in fluid-saturated granular medium, Ph.D. thesis, University of Cambridge, 2013.

[8] K. Kumar Soundararajan, Multi-scale multiphase modelling of granular flows, Ph.D. thesis, University of Cambridge, 2014.

[9] C. Mast, P. Arduino, P. Mackenzie-Helnwein, G. R. Miller, Simulating granular column collapse using the material point method, Acta Geotechnica (2014).

[10] W. Solowski, S. W. Sloan, Modelling of sand column collapse with material point method, in: G. N. Pande, S. Pietruszczak (Eds.), ComGeo III 2013, volume 553, 2013, pp. 698–705.

[11] W. Solowski, S. W. Sloan, Evaluation of material point method for use in geotechnics, International Journal for Numerical and Analytical Methods in Geomechanics 39 (2015) 685–701.

[12] S. Utili, T. Zhao, G. Houlsby, 3D DEM investigation of granular column collapse: Evaluation of debris motion and its destructive power, Engineering Geology 186 (2015) 3–16.

[13] D. Liang, X.-Z. He, A Comparison of Conventional and Shear-Rate Dependent Mohr-Coulomb Models for Simulating Landslides, Journal of Mountain Science 11 (2014) 1478–1490.

[14] E. Fern, K. Soga, The role of constitutive models in MPM simulations of granular column collapses, Acta Geotechnica published (2016).

[15] M. Jefferies, Nor-Sand : a simple critical state model for sand, Géotechnique 43 (1993) 91–103.

[16] A. Yerro, E. Alonso, N. Pinyol, The material point method for unsaturated soils, Géotechnique 65 (2015) 201–217.

[17] K. Soga, E. Alonso, A. Yerro, K. Kumar, S. Bandara, Trends in large-deformation analysis of landslide mass movements with particular emphasis on the material point method, Géotechnique 66 (2016) 248–273.

[18] E. Fern, D. J. Robert, K. Soga, Modeling the stress-dilatancy relationship of unsaturated silica sand in triaxial compression tests, Journal of Geotechnical and Geoenvironmental Engineering accepted (2016).

[19] K. H. Roscoe, J. B. Burland, On the generalised stress-strain behaviour of 'wet' clay, in: J. Heyman, F. Leckie (Eds.), Engineering plasticity, Cambridge University Press, Cambridge, 1968, pp. 535–609.

[20] E. Alonso, A. Gens, A. Josa, A constitutive model for partially saturated soils, Géotechnique 40 (1990) 405–430.

[21] K. H. Roscoe, A. N. Schofield, Mechanical behaviour of an idealised wet clay, in: 2nd European Conference on Soil Mechanics and Foundation Engineering, Wiesbaden, 1963, pp. 47–54.

[22] E. Fern, Constitutive modelling of unsaturated sand and its application to large deformation modelling, Ph.D. thesis, University of Cambridge, 2016.

[23] A. N. Schofield, P. Wroth, Critical State Soil Mechanics, 2nd ed., McGraw-Hill, London, 1968.

[24] K. H. Roscoe, A. N. Schofield, C. P. Wroth, On the yielding of soils, Géotechnique 8 (1958) 22–53.

[25] D. Taylor, Fundamentals of soil mechanics, Wiley, New York, 1948.

[26] R. Nova, A constitutive model for soil under monotonic and cyclic loading, in: G. N. Pande, C. Zienkiewicz (Eds.), Soil mechanics - transient and cyclic loading, Wiley, Chichester, 1982, pp. 343–373.

[27] M. Bolton, The strength and dilatancy of sands, Géotechnique 36 (1986) 65–78.

[28] R. W. Boulanger, Relating to relative state parameter index, Journal of Geotechnical and Geoenvironmental Engineering 129 (2003) 770–773.

[29] J. Mitchell, K. Soga, Fundamentals of Soil Behavior, 3rd ed., John Wiley & Sons, Hoboken, 2005.

[30] C. P. Wroth, R. H. Bassett, A StressStrain Relationship for the Shearing Behaviour of a Sand, Géotechnique 15 (1965) 32–56.

[31] F. Tatsuoka, M. Sakamoto, T. Kawamura, S. Fukushiima, Strength and deformation characteristics of sand in plane strain compression at extremely low pressures., Soils and Foundations 26 (1986) 65–84.

[32] K. H. Roscoe, The Influence of strains in soil mechanics, Géotechnique 20 (1970) 129–170.

[33] P. W. Rowe, The Stress-Dilatancy Relation for Static Equilibrium of an Assembly of Particles in Contact, in: Proceedings of the Royal Society A: Mathematical, Physical and Engineering Sciences, volume 269, The Royal Society, 1962, pp. 500–527.

[34] Y. Dafalias, M. T. Manzari, A critical state two-surface plasticity model for sands, Géotechnique 47 (1997) 255–272.

[35] K. Been, M. Jefferies, A state parameter for sands, Géotechnique 35 (1985) 99–112.

[36] A. Zhou, D. Sheng, An advanced hydro-mechanical constitutive model for unsaturated soils with different initial densities, Computers and Geotechnics 63 (2015) 46–66.

[37] F. Darve, G. Servant, F. Laouafa, H. Khoa, Failure in geomaterials: continuous and discrete analyses, Computer Methods in Applied Mechanics and Engineering 193 (2004) 3057–3085.

[38] D. Robert, Soil-Pipeline Interaction in Unsaturated Soils, Ph.D. thesis, University of Cambridge, 2010.